IEEE Access
Multidisciplinary | Rapid Review | Open Access Journal

Received 25 December 2023, accepted 2 January 2024, date of publication 8 January 2024,
date of current version 16 January 2024.

Digital Object Identifier 10.1109/ACCESS.2024.3351106

RESEARCH ARTICLE

An Efficient Protection Scheme Against Single-Phasing Fault for Three-Phase Induction Motor

AHMED DAWOOD[1], MOHAMED A. ISMEIL[2], (Member, IEEE), HANY S. HUSSEIN[2], (Senior Member, IEEE), B. M. HASANEEN[1], AND A. M. ABDEL-AZIZ[3]

[1]Department of Electrical Power and Machines Engineering, Faculty of Engineering in Qena, Al Azhar University, Qena 83523, Egypt
[2]Department of Electrical Engineering, Faculty of Engineering, King Khalid University, Abha 61411, Saudi Arabia
[3]Electrical Engineering Department, Faculty of Engineering in Cairo, Al Azhar University, Nasr City 11611, Egypt

Corresponding author: Ahmed Dawood (ahmeddawood.2038@azhar.edu.eg)

This work was supported by the Deanship of Scientific Research at King Khalid University through the Large Group Research Project under Grant RGP2/179/44.

ABSTRACT The loss of one phase of a three-phase Induction Motor (IM) is one of the main causes of motor failure due to overheating. Several protection devices protect IM against this fault, but the majority of conventional devices lack a thorough classification of this type of fault. So, this paper introduces a high-efficiency protection scheme to detect and classify in detail 15 types of faults that can occur due to a phase loss of a three-phase IM. These faults are classified according to the defective phase, fault location either from the power source or beyond the relay point, and motor action modes (standstill mode, transient mode, and steady state mode). One of the advantages of the presented protection method is that it is suitable for many motors because the inputs to the proposed scheme are the per-unit values of both RMS line-line voltages and line currents. The proposed scheme has been validated and tested using MATLAB Simulink under normal conditions and different faults for phase loss, during and after disconnecting the motor, and after pushing the restart button. The simulation results show that the proposed scheme behaves with high efficiency and it is able to detect and classify correctly the phase loss faults for three-phase IM within 1.5 cycles (30 ms) of the fault inception. Thus, the proposed scheme can be used as a simple and reliable scheme in the protection system of a 3-phase IM to detect and classify the different types of phase loss faults.

INDEX TERMS Induction motor, neural networks, phase loss fault, MATLAB/Simulink, fault diagnosis.

I. INTRODUCTION

One of the most popular devices for converting electrical energy into mechanical energy in industrial applications is the three-phase induction motor (IM) [1]. This is mainly, because it requires less maintenance [2]. In addition, it is dependable and durable in harsh situations, and quickly adapts to various loading conditions [1], [2], [3]. Despite these attractive features, a 3-phase IM can be subjected to many mechanical and electrical failures. A phase loss, also known as open phase, phase failure, or single phasing, is one of the most common failures of a three-phase IM [4]. This type of fault could be caused by a wide variety of factors, such as a blown fuse, broken or damaged wires, open switches, eroded or oxidized contacts, mechanical damage, melted conductors, etc. [5], [6], [7].

When a 3-phase motor is started with only two phases, it will make a humming sound and be unable to start rotation because it lacks the necessary starting torque [8]. Unless it is not previously tripped under a single-phasing fault, it will draw enough current from healthy phases to drive the load [5], [7], [9]. While a phase loss in a running motor may not immediately cause damage or failure, unless it is detected, it may force equipment to operate under stress and lead to

The associate editor coordinating the review of this manuscript and approving it for publication was Lei Shu.

overheating, which could eventually burn the motor windings [7], [10]. When an IM loses one of its phases, it is subjected to the most severe possible voltage imbalance. This forces IM to draw a higher current, which results in asymmetrical losses. Additionally, the IM stator windings experience thermal overload, which leads to insulation damage [8], [11].

According to renowned standard organizations, 30% of motor failures are due to insulation failure and 60% to overheating [8], [12]. It is estimated that 44% of failures can be attributed to single-phasing and overloading [8].

According to some research on the effect of voltage imbalance on the motor, a simple change of 3% in voltage imbalance causes the temperature to rise by 25% [11], [13]. When a motor is fully loaded, the value of unbalanced phase current is (6–10) times the percentage value of unbalanced voltage at the terminals [6], [14]. A phase loss distorts the voltage imbalance significantly [5].

In addition, the phase loss fault supplies the motors with negative series currents, which lead to the production of parasitic magnetic fields, decreasing the torque, and then causing overheating and serious effects [11], [15].

The vast majority of the protection devices for motors that are widely used, such as thermal overload relays or circuit breakers, are not designed to detect single-phasing failures [9]. If one of the three phases of a lightly loaded three-phase induction motor (70% of full-load currents) is missing, the phase current value increases by the square root of three ($\sqrt{3}$). Because of this, the amount of current drawn will be about 20% higher than indicated on the nameplate for full-load current. If the overload protection is set at 125% of the motor nameplate, the motor can be damaged by circulating currents [7], [9].

In order to protect the motor from an open phase failure, various protection devices have been developed, but the three-phase monitor relay, also known as a phase failure relay, is the hardware that is most frequently used to prevent single phasing in the various ranges of the low and middle power of electrical drives [4]. In the event of a problem, the relay energizes the protected equipment and may notify the monitoring system. Various devices for protecting against this fault have been studied [11].

Many engineers have developed software techniques to detect phase loss faults in 3-phase motors. This makes it possible to perform the right steps at the proper time, thus preventing the effects of such a severe failure. Several studies have been carried out on the topic of three-phase motor protection against single-phasing fault [16], [17], [18], [19], [20], [21], [22], [23], [24].

Recent trends in the motor protection field are moving towards using digital relays based on microprocessors. These relays have many benefits compared over electromagnetic ones in terms of accuracy, response speed, and reliability [25]. The most effective methods used to protect motors are techniques based on artificial intelligence due to their high reliability and low cost [26]. According to the type of signal used in the analyses, phase loss detection algorithms can be broadly classified into three categories: voltage, current, and combinations of them. Considering that current signals are more common due to the absence of current in the faulty phase and the presence of currents in the other two healthy phases. Simultaneously, the detected voltage may fail to identify phase loss after the sensor location. Additionally, many low-cost systems lack the voltage sensors required for detecting open phases. The third class of algorithms, which uses currents and voltages, often employs motor models for estimation and diagnosing the phase loss based on the data from these models. Phase loss detection algorithms can also be categorized into slow and fast methods according to the duration of fault detection from the time of its occurrence. It is well known that fast phase loss detection is the best method, but it is not easy in many different systems due to several different factors, such as high signal noise, distorted input voltage, etc [4].

In [27], the authors used the zero current technique, known for its fast identification of phase loss faults. They applied a second-order filter to each phase current to detect zero current. This filter monitored the rate of change of the current, enabling the detection of faults where the current was expected to rapidly decrease to zero. Nonetheless, this approach is challenging to fine-tune and computationally demanding, which negates its primary benefits. Additionally, there is no information available about its performance during transient periods.

The article [28] presented the application of the direct-quadrature (DQ) current oscillations method for phase loss detection. The authors used a specific characteristic to identify faults: under normal operating conditions for the motor, the direct and quadrature currents remain relatively stable, but in the event of a lost phase, these currents start oscillating, allowing for easy detection. While this method offers the benefit of rapid fault detection, it is susceptible to the influence of the measurement noise.

The middle current detection method, which is known for its fast phase loss fault detection, is discussed in [29] and [30]. This method offers several advantages. Firstly, it is capable of working effectively with noisy signals from the sensed currents. Additionally, it demonstrates stability during transient periods and load variations without generating false fault detections. Furthermore, it excels at handling highly distorted currents, where other methods often fail. While the computational complexity of this algorithm is slightly higher compared to the previously discussed methods, it remains relatively straightforward. The tuning process for this algorithm is not difficult and can be quickly performed.

The authors of [31], [32], [33] used a method called average phase currents. This method is similar to the zero-current detection methods, but it analyses the average current over the fundamental period. In [32], there was a small improvement made to this technique. The authors added a fuzzy-logic controller to make the recognition of faulty conditions faster and

TABLE 1. Comparison of the detection methods of the phase loss fault.

The detection Method	Computational Complexity	Tuning	Detection Speed	Sensitivity to	Reliability
Zero current	Simple	Easy	Fast	Measurement noise	Medium
DQ current oscillations	Simple	Medium	Fast	Measurement noise	Medium
Middle current detection	Simple	Easy	Fast	----	High
Average phase currents	Simple	Easy	Slow	Measurement noise, Load variation	Medium
Comparison with expected shape	Complex	Difficult	Slow	Load variation	Low
Discrete Fourier transformation	Complex	Medium	Slow	Measurement noise	High
Current zero sequence	Medium	Medium	Slow	----	Low

more reliable. They claimed that using fuzzy logic improved the reliability and stability of fault detection. However, the experimental results didn't cover situations where the speed changes suddenly or where there are variations in the load during a mechanical revolution. In those cases, the average phase current may not be zero. The advantages of the current averaging method are that it has a simple structure and is easy to adjust. However, algorithms based on this method also have a few disadvantages. They are slow because they need one period of time to average the current, and they are sensitive to noise, although not as much as the zero current detection method.

Another way to detect phase loss faults is by comparing the shape of the stator currents to what is expected. This method examines the waveform of the currents and identifies a fault if there is a noticeable difference from the expected pattern. The comparison method was explored in [34] and [35], where various criteria were proposed for analyzing the current waveform. However, this method has some drawbacks. It can be challenging to implement and fine-tune, and it is not effective with distorted currents. Also, its reliability is generally low.

In [36], the authors used the method of Discrete Fourier Transformation (DFT) or Fast Fourier Transformation (FFT), which is popular method for detecting signal distortion. Since an open phase can cause significant distortions in currents and voltages, analyzing the signals using DFT can help identify this type of failure. One advantage of this approach is its simplicity and ease of tuning in certain drive systems. Additionally, this method can be employed to detect other faults and differentiate between them [37]. However, the DFT-based method cannot solve the noisy signal problem in measurements.

In [38], a method called the current zero sequence was suggested to detect open-phase faults in a delta-connected motor. The authors examined how the motor behaves when there is a fault and identified the fundamental component of the zero-sequence current. Under normal conditions, this component is almost zero, but it increases when there is a fault. To detect open-phase fault, they compare this component with a threshold value.

The performance and implementation are summarized in Table 1, based on the discussions mentioned earlier.

Accordingly, it is clear that many researchers have presented a variety of methods for detecting single-phase loss faults, but most of them lack the classification of this type of fault. So in our article, a high-efficiency protection scheme based on ANN is proposed to detect and classify in detail 15 types of phase loss faults for three-phase IM. These faults are classified according to the unhealthy phase, fault location either from the power source or beyond the relay point, and motor action modes (standstill mode, transient mode, and steady state mode). Thus, this detailed classification help the maintenance team to repair the fault quickly after its occurrence. When the motor is in standstill mode, detection of the loss of one of the phases from the source is important to avoid running the motor with only two phases without rotation, which causes high currents to pass through the two healthy phases. Also, one of the advantages of the presented method is that it is suitable for many motors because the inputs to the proposed scheme are the per-unit values of the RMS line-line voltages and line currents. Thus, the ANN-based proposed scheme can be implemented as a simple and reliable solution for integration into the overall protection system of a three-phase induction motor, enabling the detection and classification of various phase loss faults.

II. DESCRIPTION OF THE STUDIED SYSTEM

The studied system diagram is shown in Fig.1. This system has six main parts: the power source, 3-ph motor, 3-ph breaker, measurement unit, cables, and the protective relay using the proposed scheme. The measurement unit is used to step down the voltages and currents of the 3-ph motor to be compatible with the protective relay.

In Fig. 1, we can see how the phase loss fault occurs and its different types considered in this research. Phase loss fault refers to the loss of one of the phases (A, B, or C) either from the source (location 1 in Fig. 1) or after the relay location (location 2 in Fig. 1). The phase loss fault can occur when the 3-ph motor is running in steady-state mode or transient mode or when it is in standstill mode.

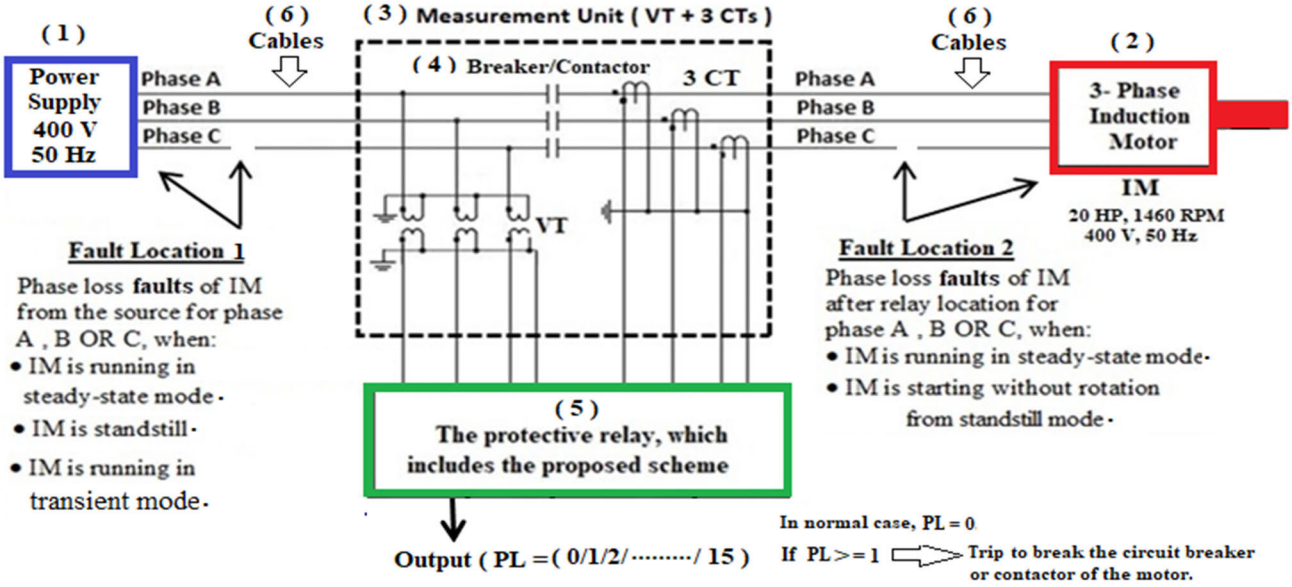

FIGURE 1. Schematic diagram of the system under study.

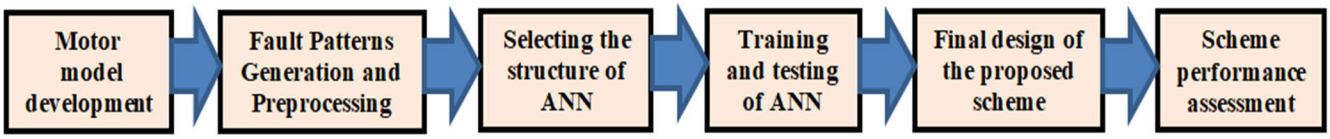

FIGURE 2. Block diagram of the workflow for designing the proposed scheme.

If there is a loss of phase while the motor is running, it should be detected, and the motor should be disconnected using a breaker to prevent overheating. When the motor is stopping, it is important to detect if one of the phases is lost from the power source to avoid starting the motor with only two phases. Starting the motor with only two phases causes high currents to flow through the remaining healthy phases.

In addition, when the three-phase induction motor is in standstill mode, the loss of one of the phases after the relay location should be detected as soon as the motor is started from standstill mode without rotation.

The proposed scheme can accurately identify and classify 15 types of phase loss faults based on factors such as the unhealthy phase, fault location, and motor action modes (standstill, transient, and steady-state) as follows:

- ❖ Loss of phase "A" from the source side when the motor is running in steady-state mode.
- ❖ Loss of phase "B" from the source side when the motor is running in steady-state mode.
- ❖ Loss of phase "C" from the source side when the motor is running in steady-state mode.
- ❖ Loss of phase "A" after the relay point when the motor is running in steady-state mode (For example, a phase loss fault occurs in the motor winding or in the cable between the relay and the motor).
- ❖ Loss of phase "B" after the relay point when the motor is running in steady state mode.
- ❖ Loss of phase "C" after the relay point when the motor is running in steady state mode.
- ❖ Loss of phase "A" from the source side when the motor is running in transient mode.
- ❖ Loss of phase "B from the source side when the motor is running in transient mode.
- ❖ Loss of phase "C" from the source side when the motor is running in transient mode.
- ❖ loss of phase "A" after the relay point when the motor starts in transient mode without rotation.
- ❖ loss of phase "B" after the relay point when the motor starts in transient mode without rotation.
- ❖ loss of phase "C" after the relay point when the motor starts in transient mode without rotation.
- ❖ Loss of phase "A" from the source side when the motor is in standstill mode.
- ❖ Loss of phase "B" from the source side when the motor is in standstill mode.
- ❖ Loss of phase "C" from the source side when the motor is in standstill mode.

III. RESEARCH METHOD

The work stages for designing the proposed scheme based on Artificial Neural Network (ANN) to detect and classify the phase loss faults of IM consist of six stages as follows:

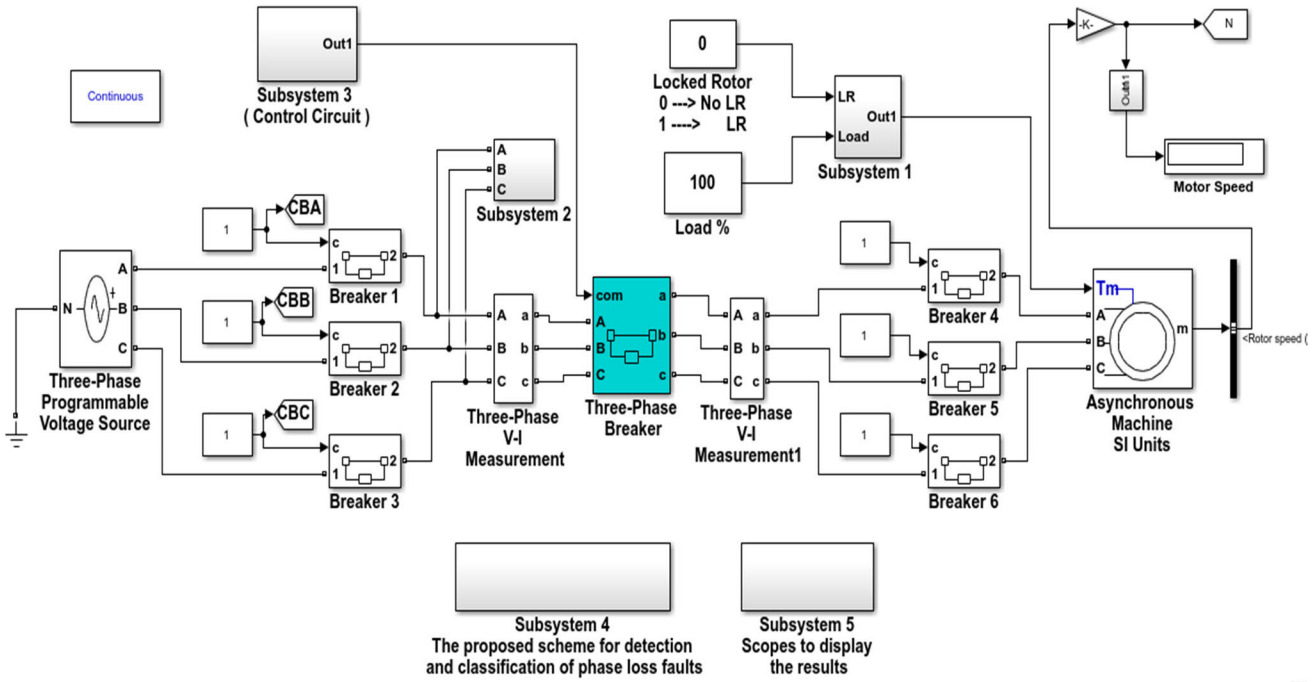

FIGURE 3. The system under study represented in MATLAB Simulink.

- Motor model development
- Fault patterns generation and preprocessing
- Selecting the structure of ANN
- Training and testing of ANN
- Final design of the proposed scheme
- Proposed scheme performance assessment

Figure 1 shows the work stages for designing the proposed scheme based on ANN to detect and classify the phase loss faults of 3-ph IM. These stages are explained in detail in Subsections A, B, C, D, E and F.

A. MOTOR MODEL DEVELOPMENT

In this paper, the studied system model, which includes a three-phase IM, has been built using MATLAB/Simulink software. The model is employed as a simulation platform to simulate the motor's performance under various types of phase loss faults. The study is carried out on a model of the three-phase induction motor models found in the MATLAB/Simulink environment. The research is based on a three-phase squirrel cage IM, 400 V, 15 kW (20 HP), 1460 rpm, 50 Hz, with star-connected windings. The data of a three-phase induction motor, including the values of stator resistance, stator inductance, rotor resistance, and rotor inductance, are given in Table 2.

Figure 3 shows the diagram of the system under study in MATLAB/Simulink, which consists of many different types of blocks. One block is called "Three-phase programmable voltage source," which is used to simulate the power supply of the three-phase motor fed at 400 V at 50 Hz. A block called "Asynchronous Machine" is used to simulate the performance of a 3-ph motor. A block called a "Three-Phase Breaker" is used to start and stop the motor. Two blocks, one called "Three-Phase V-I Measurement" is used to measure line-line voltages, and the second called "Three-Phase V-I Measurement1" is used to measure line currents of the motor. Two groups of blocks, one called "Circuit Breaker 1, 2, and 3", are used to simulate the phase loss fault from the power source, and the other called "Circuit Breaker 4, 5, and 6" are used to simulate the phase loss fault after the relay location (i.e., the simulation of a phase loss fault occurs in the motor winding or in the cable between the relay point and the motor, or if there is a problem with the motor connection box). A block called "subsystem 1" is designed for two reasons: the first is to run the motor with different loads as a percentage of the full load, and the second is to block the motor rotor

TABLE 2. Motor data used in MATLAB/Simulink for the studied system.

Motor Parameters	Value	Unit
Nominal power	20	HP
RMS Line to Line voltage	400	V
Motor Speed	1460	RPM
Frequency	50	Hz
Pole pairs	2	---
Stator resistance (Rs)	0.2147	Ω
Stator inductance (Ls)	0.000991	H
Rotor resistance referred to stator (Rr')	0.2205	Ω
Rotor inductance referred to stator (Lr')	0.000991	H
Mutual inductance (Lm)	0.06419	H

TABLE 3. Target values of the outputs of the NN according to the type of phase loss.

Fault type description	Target of ANN			
	A	B	C	T
Phase A is cut off from supply when the motor is running in steady state mode or transient mode or when the motor is in standstill mode.	1	0	0	0
Phase B is cut off from supply when the motor is running in steady state mode or transient mode or when the motor is in standstill mode.	0	1	0	0
Phase C is cut off from supply when the motor is running in steady state mode or transient mode or when the motor is in standstill mode.	0	0	1	0
Phase A is cut off after the relay point when the motor is running in steady-state mode or at the start of the motor with no rotation.	1	0	0	1
Phase B is cut off after the relay point when the motor is running in steady-state mode or at the start of the motor with no rotation.	0	1	0	1
Phase C is cut off after the relay point when the motor is running in steady-state mode or at the start of the motor with no rotation.	0	0	1	1
Normal case (no phase loss fault)	0	0	0	0

when it starts under a phase loss failure. A block called ''subsystem 2'' is designed to simulate a phase loss failure from the power source when the ''three-phase breaker'' is disconnected and the motor is in standstill mode. A block called ''subsystem 3'' is designed to simulate the control circuit of the motor to generate start and restart signals and also to generate a signal to stop the motor when a phase loss fault occurs. A block called ''subsystem 4'' is designed to simulate the proposed scheme for the detection and classification of phase loss faults. A block called ''subsystem 5'' is used to display the results of the proposed scheme.

B. FAULT PATTERNS GENERATION AND PREPROCESSING

Preprocessing is a valuable technique that considerably reduces the size of the NN and increases the training process's performance and speed. After designing the proposed system in Simulink of MATLAB as previously described in Section 2.1, a simulation will be made to collect the data required to train the proposed NN. The input signals for ANN were sampled at a sampling frequency of 1 kHz. The data collected during the simulation process are the RMS values of line-line voltages and line currents. Then, these measured values are converted to per-unit values as follows:

- The per-unit values of RMS line-line voltages are based on the rated line-line voltage of the motor.
- The per-unit values of RMS line currents are based on the rated current of the motor.

The simulation process in Simulink of MATLAB will be done to collect data when the motor is in normal operation and when it experiences a loss of one of the three phases while the motor is running in transient mode or steady state mode. In addition, data is collected when one of the phases of the source is lost while the motor is in standstill mode to prevent motor operation under this condition. For each simulated fault case, 20 samples were collected after one cycle from fault inception in order to generate a training data set for ANN. The data sets (normal and fault patterns) are collected at variant loading conditions (0–100%) of the full load.

C. FAULT STRUCTURE OF THE ANN FOR FAULT DETECTION AND CLASSIFICATION TASKS

Following the process of selecting the inputs to the NN, the next stage is to form the structure of the ANN-based fault detector and classifier for the phase loss fault of the three-phase motor. A multi-layer feed-forward NN is chosen for this research. It is necessary, in the design stage of the NN, to take into account the determination of the size and the ideal structure of the NN. The structure selection of the NN depends on the classification problem involving fault patterns, which ultimately relate to the number of input and output neurons. In this study, the per-unit values of RMS line-line voltages and RMS line currents were chosen as inputs to the NN, so the total number of neurons in the input layer for the ANN is 6. The number of neurons in the output layer is 4. The target values of the outputs of the NN are selected according to the fault type as listed in Table 3. This classification, which consists of six categories, is done using the NN. At the end of the proposed scheme, 15 types will be classified according to the motor case during the fault occurrence.

D. TRAINING AND TESTING OF ANN

After determining the number of neurons in the input and output layers of the proposed NN, the next step is to train the NN with the previously prepared fault patterns. The datasets collected are divided into 80% for training, 10% for testing, and 10% for validation. After a series of experiments with different networks by changing the number of hidden neurons in the hidden layer, it was obtained that the highest performance could be achieved by employing a single hidden layer containing 10 neurons. Thus, the final structure of the ANN is a feed-forward neural network with 6 input neurons, 10 hidden neurons, and 4 output neurons. Both the hidden layer and the output layer have used the ''tangent sigmoid'' transfer function. The ANN was trained using the Levenberg–Marquardt training algorithm. As shown in Fig. 4, the learning strategy converges rapidly, and the Mean Squared

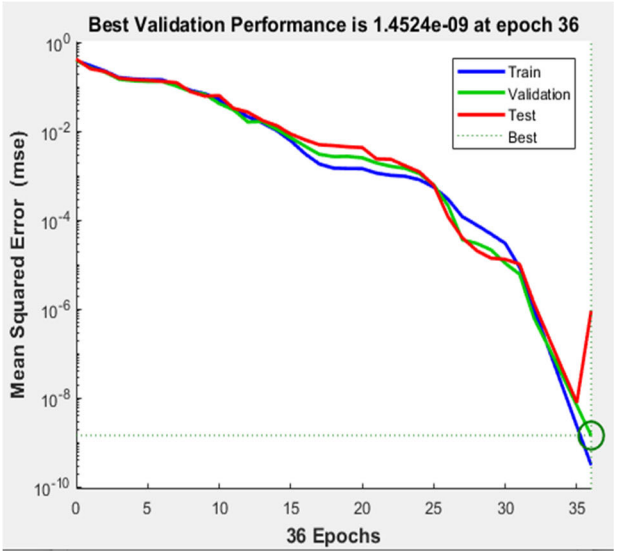

FIGURE 4. Training of the ANN Model, giving the MSE.

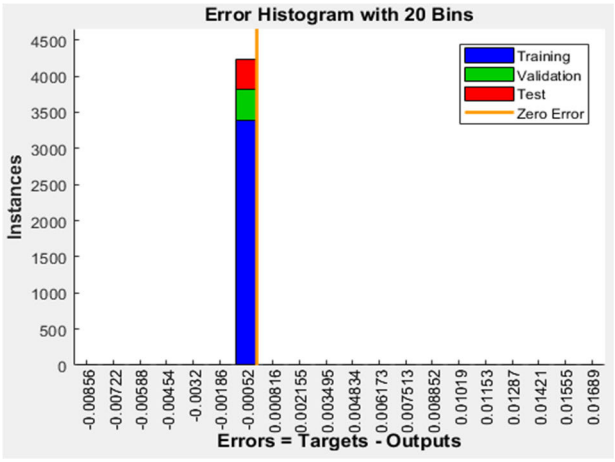

FIGURE 5. Error histogram of the NN training.

Error (MSE) drops to 1.4524 e-9 in 36 epochs. The error histogram diagram of the neural network training is shown in Fig. 5.

Following the training of the NN, it is required to design the final proposed scheme. Therefore, the following subsection explains the final proposed scheme design based on this neural network.

E. FINAL DESIGN OF THE PROPOSED SCHEME

After designing the NN, which classifies six categories of phase loss faults for a 3-ph induction motor, the final design of the proposed scheme is implemented in this part. Figure 6 shows the flowchart loop of the final design of the proposed scheme.

In step 1 (the beginning of the scheme), the output value of the algorithm (PL) is set to zero. In step No. 2, the user enters the motor data (such as the rated line-line voltage and rated line current) and the measuring device data (such as the ratio of the voltage transformers and the current transformers).

In step 3, the RMS samples for line-line voltages and line currents are read from the measuring devices, as well as the case of the ''Reset'' push-button (0/1).

In step 4, the measured voltages and currents are converted to per-unit values. The per-unit values of the line-line voltages are based on the motor-rated value of the line-line voltage (VAB, VBC, and VCA). The per-unit values of the line currents are based on the motor-rated value of the line current (IA, IB, and IC).

In Step No. 5, the state of the motor is determined in terms of three cases. The first case is that the motor is in standstill mode, and in this case, the value of M is set to zero. The second case is that the motor is running in transient mode, and in this case, the value of M is set to 1. The third case is that the motor is running in steady state mode, and in this case, the value of M is set to 2. In this paper, the motor case is changed from transient mode to steady state mode when the line currents are less than 1.05 per unit and the timer T1 is more than 1 cycle (20 ms). A value of 1.05 is chosen assuming a 5% overload tolerance, and the timer (T1) is used to avoid samples of current that are less than 1.05 pu at the moment of starting the motor.

In step 6, the basic algorithm based on ANN is applied to detect and classify the phase loss faults of the IM. In Step 7, the operating circuit of the motor is disconnected in the event of a phase loss failure. In step 8, the results of the proposed scheme are shown in real time with the per-unit voltages, per-unit currents, and the case of the reset push-button (0 or 1) to show how the proposed scheme works during normal operation and phase loss faults.

Then the proposed scheme goes back to step No. 3 to read the values again from the measuring devices, and the previous steps are repeated, and so on. When any fault is detected, the proposed scheme gives a trip signal to stop the motor, and the value of this fault continues over time to show the fault type until the reset push button is pressed.

Figure 7 shows the flow chart of the basic algorithm mentioned in step 6. At the start of this algorithm, when the PL value is zero or the reset push button value is one, the NN that was set up before is used. If the NN is applied, its outputs will be four values, as mentioned previously in Table No. 2. Then the NN outputs are modified as follows:

- Any output greater than 0.6 is set to 1, otherwise it is zero
- The four outputs of ANN are replaced by a single value called (PL), which expresses the fault type or normal mode with values of 3, 6, 9, 12, 15, 18, and zero, respectively, as given in Table 3.
- The output (PL) is delayed by 20 ms in case of any phase loss fault (when PL $>$ 0) to avoid any classification error, especially at the start of the normal operating period.

In the last step of the basic algorithm, the fault type is classified according to the motor operation modes. If the motor operates in steady-state mode, the fault value (PL) will be the same as previously mentioned. If the fault occurs

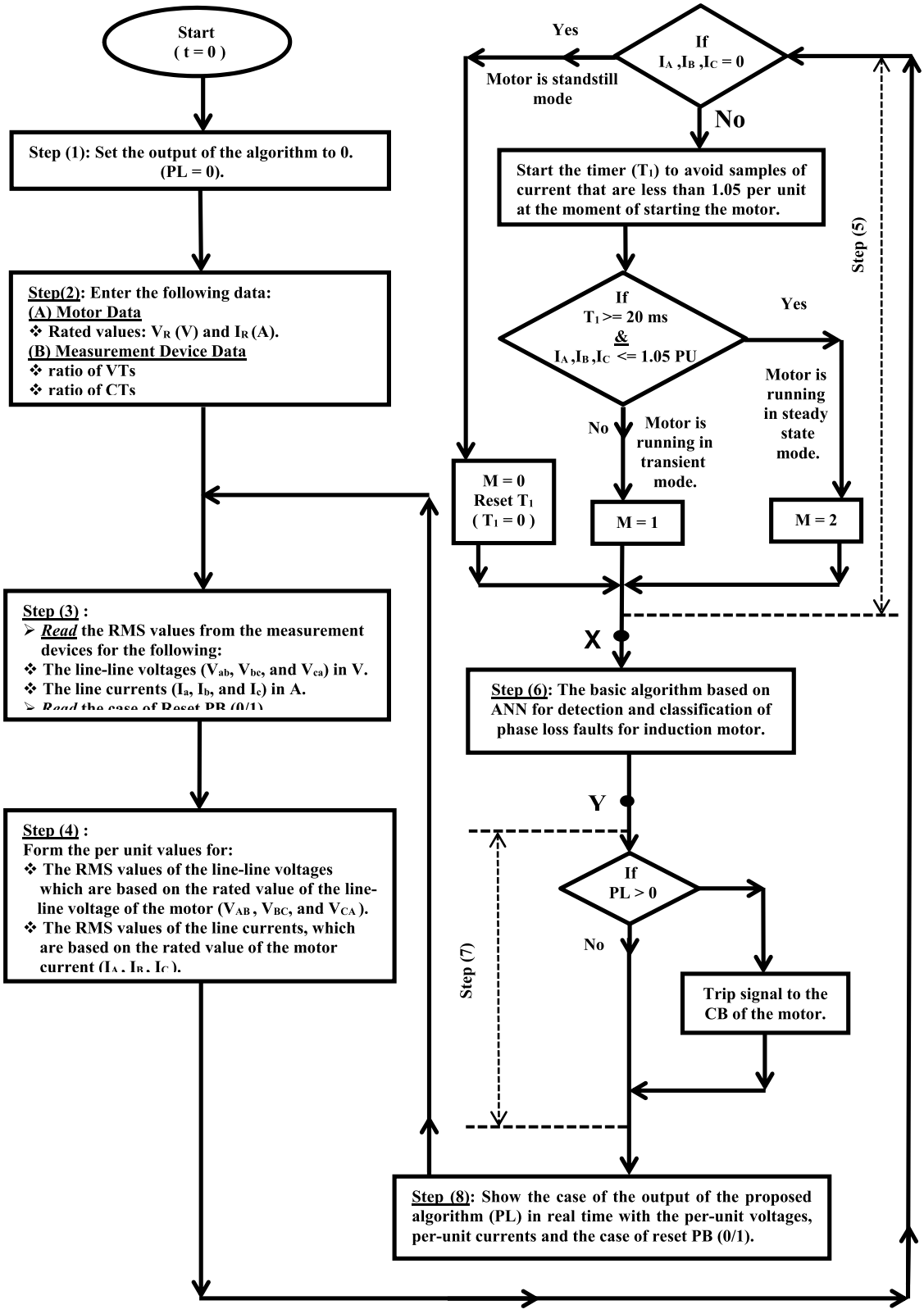

FIGURE 6. General flow chart of the proposed algorithm for detection and classification of phase loss faults for 3-phase IM.

when the motor operation is in transient mode, the fault value is reduced by 1. If the motor is in standstill mode, the fault value decreases by 2. Under normal conditions, the PL value is zero. Thus, the final classification of the proposed scheme for all faults will be according to their values as given in Table 4.

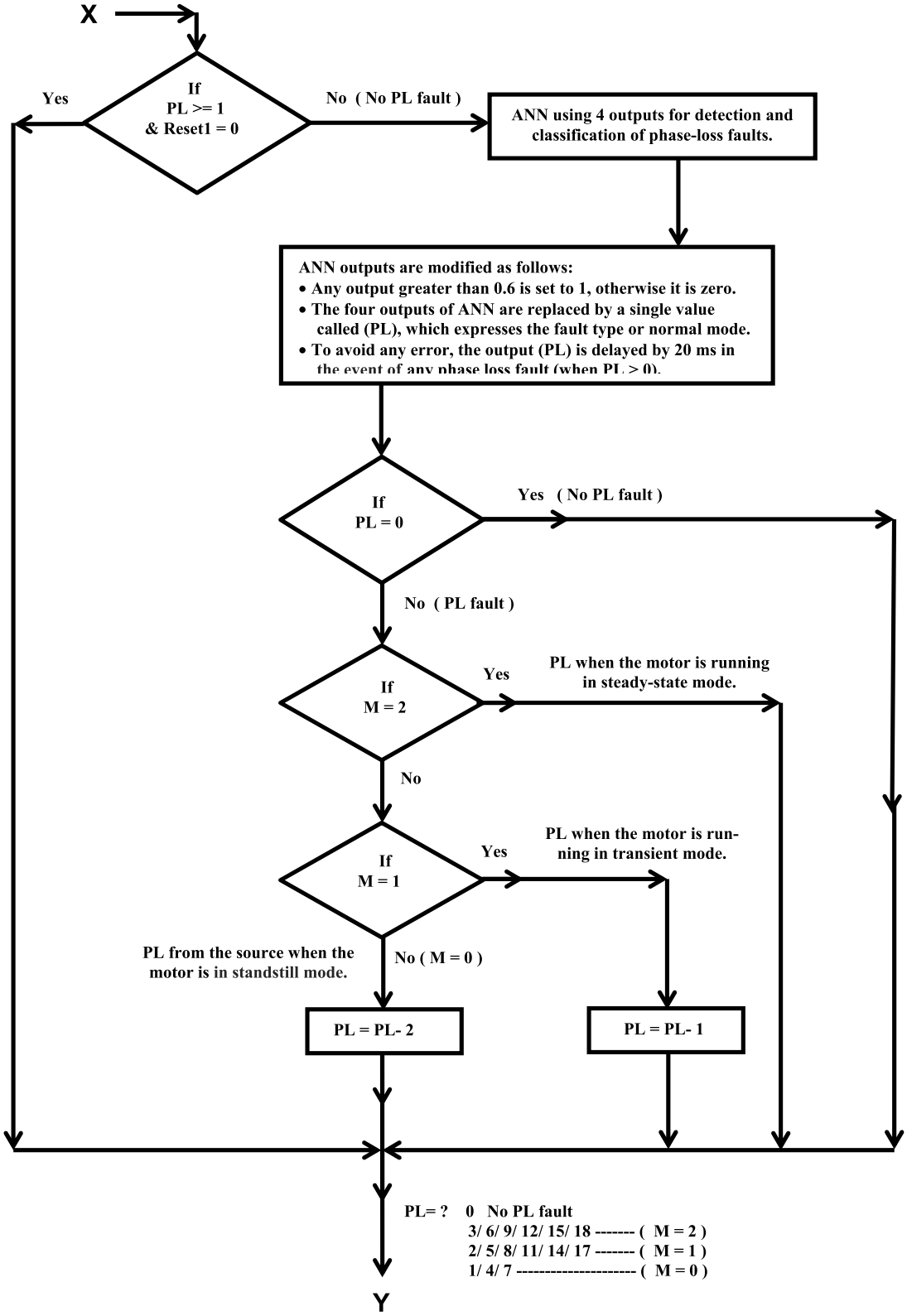

FIGURE 7. Flow chart of the basic algorithm mentioned in step 6 in Fig. 5 for detection and classification of phase loss faults (PL) of 3-phase IM.

F. RESULTS AND DISCUSSION

After designing the proposed system to detect faults caused by the loss of one of the IM phases, it must be tested in a variety of scenarios. Testing is required to validate the proposed scheme's performance in detecting motor phase failure under different operating conditions. Therefore, the proposed

TABLE 4. Description of the phase loss faults for the proposed scheme according to its output (PL).

Fault type code	The value of M during the fault occurrence	The output of the proposed scheme (PL)	Fault type description
PL1-A	2	3	Phase A is cut off from supply when the motor is running in steady state mode.
PL1-B	2	6	Phase B is cut off from supply when the motor is running in steady state mode.
PL1-C	2	9	Phase C is cut off from supply when the motor is running in steady state mode.
PL2-A	2	12	Phase A is cut off after the relay point when the motor is running in steady-state mode.
PL2-B	2	15	Phase B is cut off after the relay point when the motor is running in steady-state mode.
PL2-C	2	18	Phase C is cut off after the relay point when the motor is running in steady-state mode.
PL3-A	1	2	Phase A is cut off from the supply when the motor is running in transient mode.
PL3-B	1	5	Phase B is cut off from the supply when the motor is running in transient mode.
PL3-C	1	8	Phase C is cut off from the supply when the motor is running in transient mode.
PL4-A	1	11	Phase A is cut off after the relay point when the motor is running in transient mode.
PL4-B	1	14	Phase B is cut off after the relay point when the motor is running in transient mode.
PL4-C	1	17	Phase C is cut off after the relay point when the motor is running in transient mode.
PL5-A	0	1	Phase A is cut off from supply when the motor is in standstill mode.
PL5-B	0	4	Phase B is cut off from supply when the motor is in standstill mode.
PL5-C	0	7	Phase C is cut off from supply when the motor is in standstill mode.
---	0/ 1/ 2	0	Normal case (no phase loss fault)

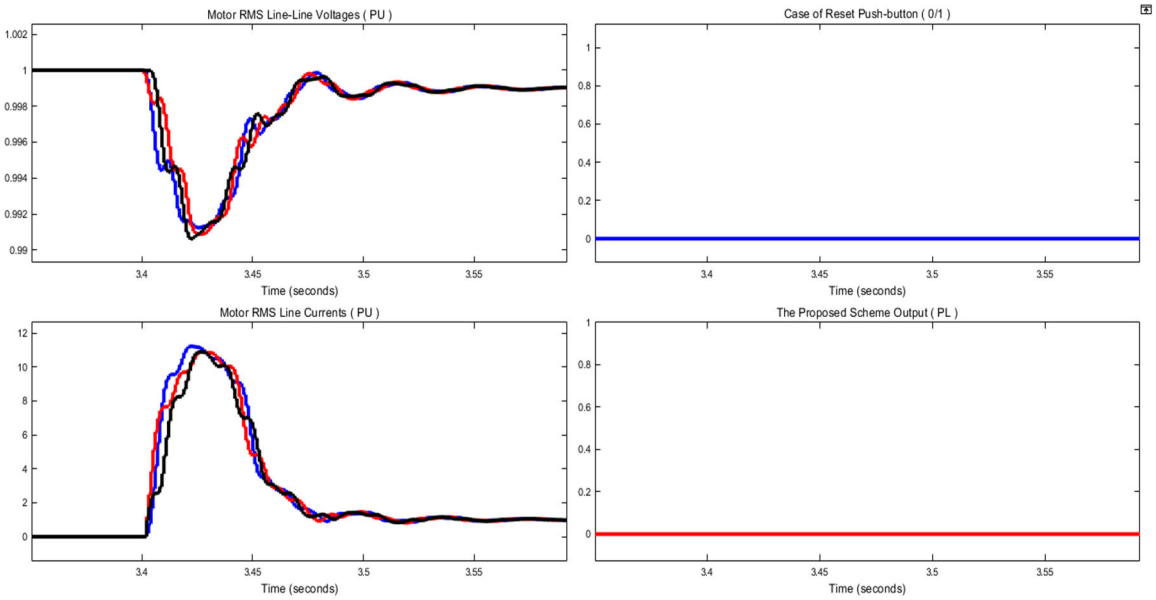

FIGURE 8. Test result of the ANN-based fault detector and classifier while the motor is running normally under full load at a time of 3.4 seconds.

scheme is tested when the motor is running normally and when any of the faults given in Table 3 happen under different loads and at different failure times, as explained below. In all simulations, the output of the proposed scheme (PL) is presented through time with the per-unit voltages, per-unit currents, and the case of the reset push-button to show how the proposed scheme works during normal operation and phase loss faults. The reset button signal generated in the simulation system is assumed to be of 1/2 cycle duration (10 ms).

1) TEST RESULTS FOR NORMAL CONDITIONS

The presented scheme is tested by running the motor under various loads without losing one of the phases. It was found that the proposed method gives efficient results, and its output is zero during the period of motor starting and during its normal rotation without any failure in case of the loss of one of the phases. Figure 8 shows one of these cases, in which the motor starts normally under full load at 3.4 seconds. It is clear from this figure that the output of the proposed method is equal to zero. Consequentially, it is not affected by the starting current of the motor, and it works without errors in this mode.

2) TEST RESULTS FOR PHASE LOSS FROM THE SOURCE WHEN THE MOTOR IS RUNNING IN STEADY- STATE

The proposed scheme is tested in many cases under various load conditions when one phase is cut off from the source while the motor is running in steady-state mode. It was found that the proposed scheme worked efficiently. Figure 9 shows

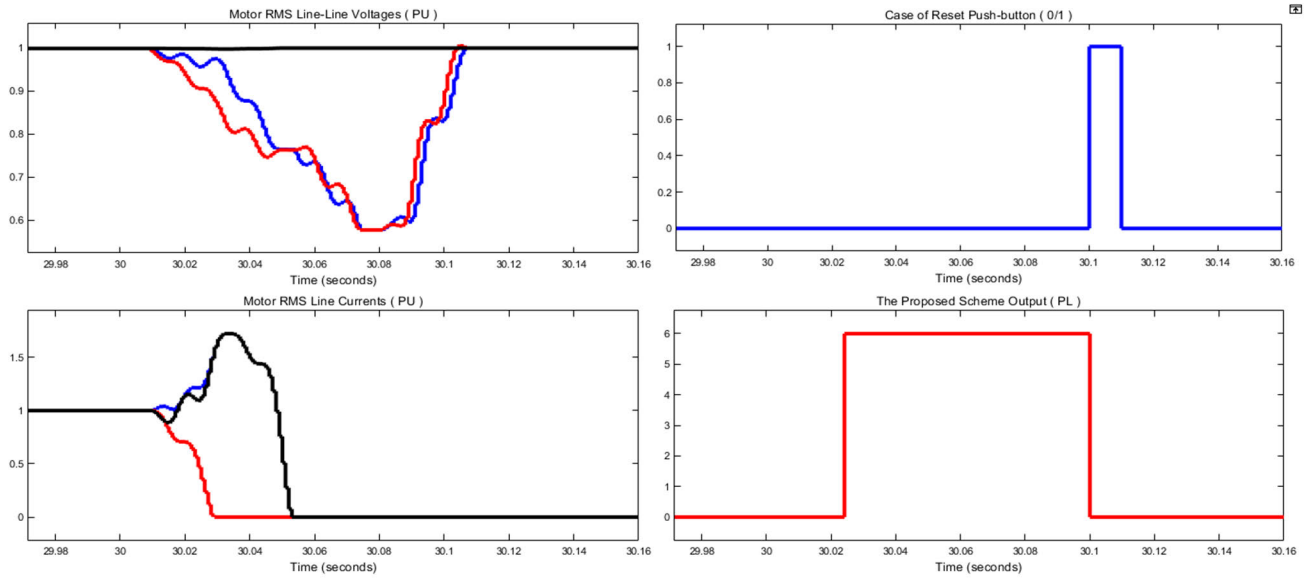

FIGURE 9. Test result of the proposed fault detector and classifier for loss of phase "B" from the source at a time of 30 seconds when the motor is running in steady-state mode under full load.

TABLE 5. Results of the proposed fault detector and classifier for one-phase loss (A, B, or C) from the source while the motor is running in steady-state mode under various load conditions.

Fault type code	Motor loading (%)	Fault inception time (Sec.)	Output of the proposed scheme (PL)	Fault detection time (Sec.)	Operation time (ms)	Fault repair time (Sec.)	Reset time (Sec.)	The scheme output after reset (PL)
PL1-A	100	10.324	3	10.345	21	10.404	10.424	0
PL1-A	90	10.420	3	10.440	20	10.500	10.520	0
PL1-A	80	20.315	3	20.335	20	20.395	20.415	0
PL1-A	70	20.615	3	20.635	20	20.695	20.715	0
PL1-A	60	30.415	3	30.435	20	30.495	30.515	0
PL1-A	50	30.525	3	30.545	20	30.605	30.625	0
PL1-A	40	40.635	3	40.656	21	40.715	40.735	0
PL1-B	100	30.000	6	30.024	24	30.080	30.100	0
PL1-B	90	10.320	6	10.343	23	10.400	10.420	0
PL1-B	80	10.425	6	10.448	23	10.505	10.525	0
PL1-B	70	20.325	6	20.348	23	20.405	20.425	0
PL1-B	60	20.635	6	20.658	23	20.715	20.735	0
PL1-B	50	30.427	6	30.450	23	30.507	30.527	0
PL1-B	40	30.625	6	30.649	24	30.705	30.725	0
PL1-C	100	10.424	9	10.452	28	10.504	10.524	0
PL1-C	90	10.320	9	10.348	28	10.400	10.420	0
PL1-C	80	20.415	9	20.443	28	20.495	20.515	0
PL1-C	70	20.525	9	20.549	24	20.605	20.625	0
PL1-C	60	30.318	9	30.341	23	30.398	30.418	0
PL1-C	50	30.423	9	30.446	23	30.503	30.523	0
PL1-C	40	40.536	9	40.559	23	40.616	40.636	0

one of these cases, which is the loss of phase "B" from the source at a time of 30 seconds when the motor is running in steady-state mode under full load. It is clear from this figure that the fault is detected and classified correctly (PL = 6) at a time of 30.024 seconds, and then the motor is stopped. Thus, the operation time for detecting and classifying the fault is 24 ms from the fault inception time. To fully illustrate the performance of the proposed scheme, the fault in the simulation is quickly repaired at 30.08 sec., and then the restart button is quickly pushed at 30.1 sec. It is clear from this figure that once the restart push-button is pushed after the fault is repaired, the output of the proposed scheme returns to its normal mode and becomes zero. Table 5 mentions all cases (21 cases) of this type of fault, which is known as codes PL1-A, PL1-B, and PL1-C, as previously given in Table 4.

3) TEST RESULTS FOR PHASE LOSS AFTER RELAY LOCATION WHEN THE MOTOR IS RUNNING IN STEADY-STATE MODE

The proposed scheme is tested for many cases under various load conditions, with one phase loss after the relay location

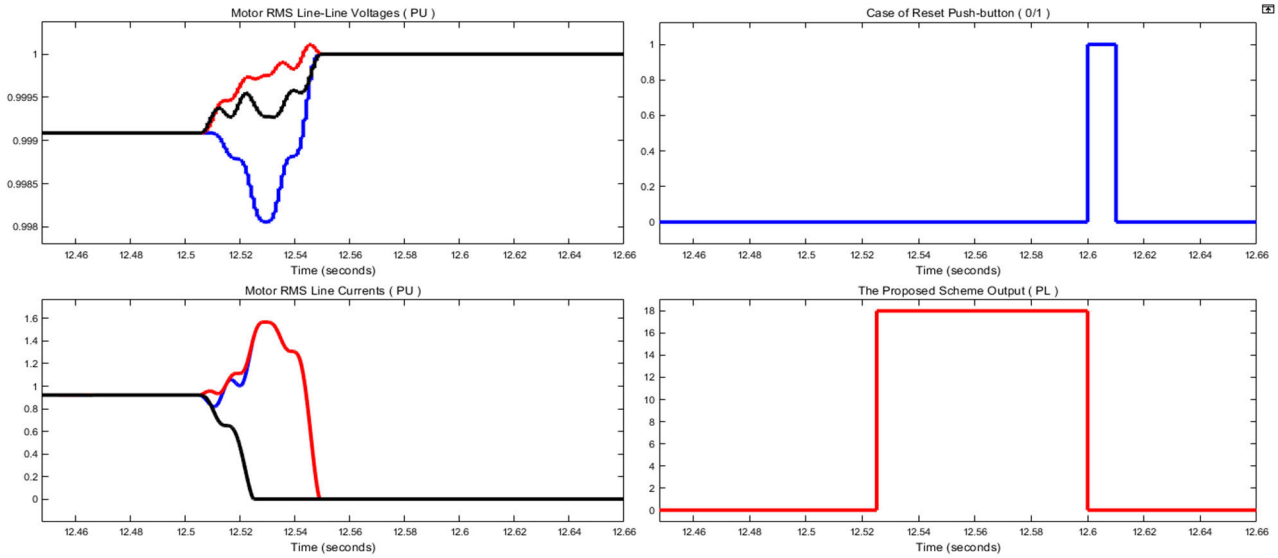

FIGURE 10. Test result of the proposed fault detector and classifier for loss of phase "C" after relay point at a time of 12.5 seconds when the motor is running in steady-state mode under 90% of full load.

TABLE 6. Results of the proposed fault detector and classifier for one-phase loss (A, B, or C) after the relay location, while the motor is running in steady-state mode under various load conditions.

Fault type code	Motor loading (%)	Fault inception time (Sec.)	Output of the proposed scheme (PL)	Fault detection time (Sec.)	The operation time (ms)	Fault repair after stopping the motor	Reset time (Sec.)	Scheme output after reset (PL)
PL2-A	100	40.315	12	40.340	25	Yes / No	40.415	0
PL2-A	90	30.427	12	30.451	24	Yes / No	30.527	0
PL2-A	85	30.625	12	30.648	23	Yes / No	30.725	0
PL2-A	75	20.325	12	20.346	21	Yes / No	20.425	0
PL2-A	65	20.635	12	20.656	21	Yes / No	20.735	0
PL2-A	55	10.320	12	10.341	21	Yes / No	10.420	0
PL2-A	45	10.527	12	10.548	21	Yes / No	10.627	0
PL2-B	100	40.325	15	40.352	27	Yes / No	40.425	0
PL2-B	90	30.457	15	30.483	26	Yes / No	30.557	0
PL2-B	85	30.645	15	30.671	26	Yes / No	30.745	0
PL2-B	75	20.335	15	20.361	26	Yes / No	20.435	0
PL2-B	65	20.634	15	20.659	25	Yes / No	20.734	0
PL2-B	55	10.323	15	10.349	26	Yes / No	10.423	0
PL2-B	45	10.547	15	10.573	26	Yes / No	10.647	0
PL2-C	100	11.424	18	11.452	28	Yes / No	11.524	0
PL2-C	90	12.500	18	12.525	25	Yes / No	12.600	0
PL2-C	85	42.315	18	42.339	24	Yes / No	42.415	0
PL2-C	75	31.427	18	31.450	23	Yes / No	31.527	0
PL2-C	65	33.625	18	33.648	23	Yes / No	33.725	0
PL2-C	55	25.325	18	25.348	23	Yes / No	25.425	0
PL2-C	45	27.635	18	27.658	23	Yes / No	27.735	0

while the motor is running in steady-state mode. It was found that the proposed method produces efficient results. Figure 10 shows one of these cases, the loss of phase "C" at a time of 12.5 seconds when the motor is running in steady-state mode under 90% of full load. It is clear from this figure that the fault is detected and classified correctly (PL = 18) at a time of 12.525 seconds, and then the motor is stopped. Thus, the operation time for detecting and classifying the fault is 25 ms from the fault inception time. It is also clear that once the restart push-button is pressed at a time of 12.6 seconds after the motor goes into standstill, the output of the proposed scheme returns to its normal mode and becomes zero. If the motor is restarted and the fault has not been repaired, then the scheme detects this fault, but at the beginning of transient mode and with a different value, as shown in sub-section III-E. Table 6 mentions all cases (21 cases) of this type of fault, which is known as codes PL2-A, PL2-B, and PL2-C, as previously given in Table 4.

4) TEST RESULTS FOR PHASE LOSS FROM THE SOURCE WHEN THE MOTOR IS RUNNING IN THE TRANSIENT MODE

The proposed scheme is tested for several cases of phase loss from the source when the motor is running at the beginning and during the transient mode. It has been found that the

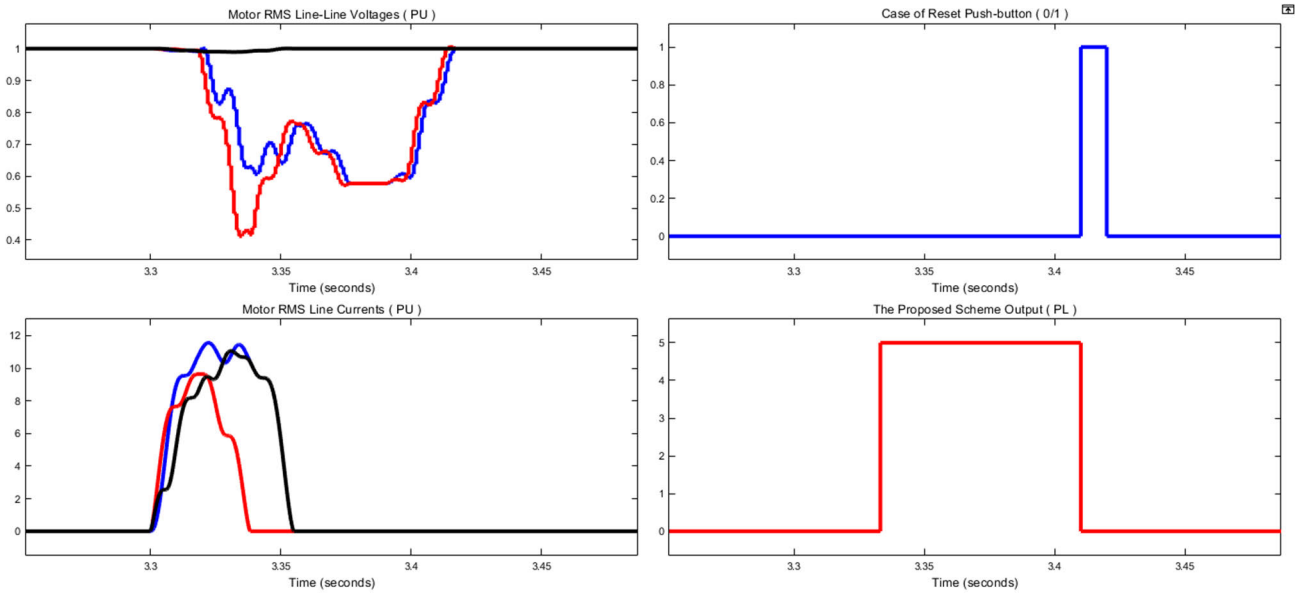

FIGURE 11. Test result of the proposed fault detector and classifier for loss of phase "B" from the source at a time of 3.31 seconds when the motor is running in the transient mode.

TABLE 7. Results of the proposed fault detector and classifier for one-phase loss (A, B, or C) from the source when the motor is running at the beginning and during the transient mode.

Fault type code	Motor starting time (Sec.)	Fault inception time (Sec.)	Output of proposed scheme (PL)	Fault detection time (Sec.)	The operation time (ms)	Fault repair time (Sec.)	Reset time (Sec.)	Scheme output after reset (PL)
PL3-A	3.30	3.310	2	3.329	19	3.39	3.410	0
PL3-A	4.20	4.200	2	4.214	14	4.280	4.300	0
PL3-A	5.30	5.310	2	5.329	19	5.390	5.410	0
PL3-A	7.20	7.220	2	7.244	24	7.300	7.320	0
PL3-A	6.27	6.270	2	6.284	14	6.350	6.370	0
PL3-A	9.20	9.220	2	9.244	24	9.300	9.320	0
PL3-A	5.20	5.200	2	5.214	14	5.280	5.300	0
PL3-B	3.30	3.310	5	3.333	23	3.390	3.410	0
PL3-B	7.20	7.200	5	7.224	24	7.280	7.300	0
PL3-B	5.30	5.310	5	5.333	23	5.390	5.410	0
PL3-B	6.20	6.220	5	6.250	30	6.300	6.320	0
PL3-B	8.20	8.200	5	8.224	24	8.280	8.300	0
PL3-B	9.27	9.270	5	9.294	24	9.350	9.370	0
PL3-B	8.20	8.220	5	8.250	30	8.300	8.320	0
PL3-C	5.20	5.200	8	5.218	18	5.280	5.300	0
PL3-C	3.30	3.313	8	3.343	30	3.393	3.413	0
PL3-C	7.27	7.270	8	7.288	18	7.350	7.370	0
PL3-C	3.30	3.314	8	3.343	29	3.394	3.414	0
PL3-C	8.27	8.270	8	8.288	18	8.350	8.370	0
PL3-C	7.30	7.313	8	7.343	30	7.393	7.413	0
PL3-C	9.20	9.200	8	9.218	18	9.280	9.300	0

proposed scheme is able to detect and classify all types of these faults correctly in 1.5 cycles (30 ms) from the fault inception time. Figure 11 shows one of these cases, where the loss of phase "B" from the source happens during the transient mode of the motor at a time of 3.31 seconds (after 10 ms from the motor starting time). It is clear from this figure that the fault is detected and classified correctly (PL = 5) at a time of 3.333 seconds, and then the motor goes into standstill mode. Thus, the operation time for detecting and classifying the fault is 23 ms from the fault inception time. To fully illustrate the performance of the proposed scheme, the fault in the simulation is quickly repaired at 3.39 sec., and then the restart button is quickly pushed at 3.41 sec. It is clear from this figure that once the restart push-button is pressed after the fault is repaired, the output of the proposed scheme returns to its normal mode and becomes zero. Table 7 gives all cases (21 cases) of this type of fault, which is known as codes PL3-A, PL3-B, and PL3-C, as previously given in Table 4.

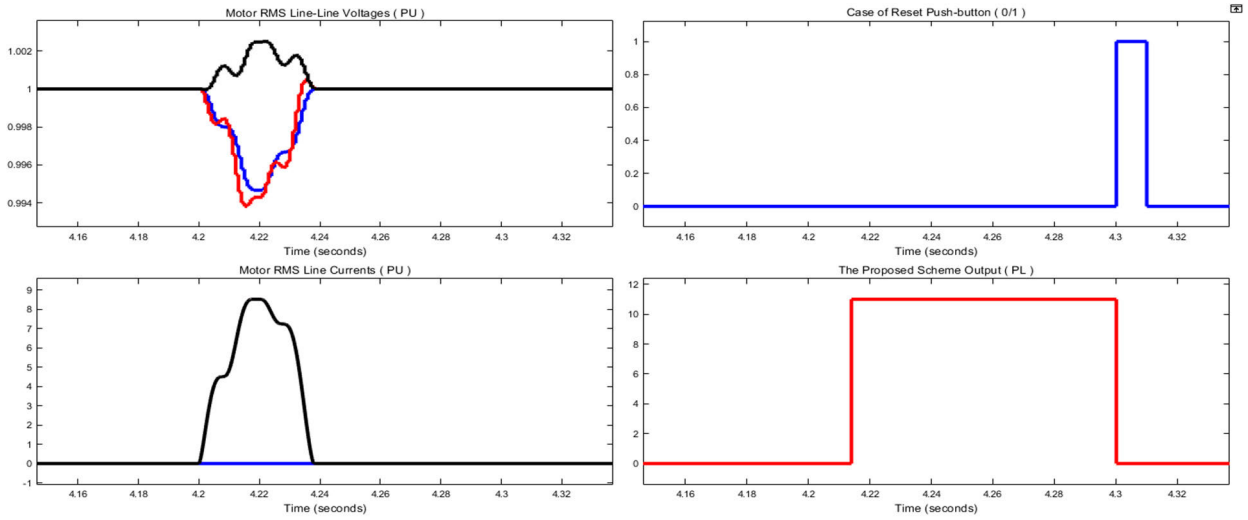

FIGURE 12. Test result of the proposed fault detector and classifier when the motor starts at a time of 4.2 seconds without rotation because of loss of phase "A" after relay location.

TABLE 8. Results of the proposed fault detector and classifier for one-phase loss (A, B, or C) after relay location when the motor is running at the beginning and during the transient mode.

Fault type code	Motor starting time (Sec.)	Fault inception time (Sec.)	Output of the proposed scheme (PL)	Fault detection time (Sec.)	The operation time (ms)	Fault repair time (Sec.)	Reset time (Sec.)	The scheme output after Reset (PL)
PL4-A	5.20	5.200	11	5.214	14	5.280	5.300	0
PL4-A	4.30	4.310	11	4.340	30	4.390	4.410	0
PL4-A	3.35	3.350	11	3.364	14	3.430	3.450	0
PL4-A	2.30	2.350	11	2.379	29	2.430	2.450	0
PL4-A	4.20	4.200	11	4.214	14	4.280	4.300	0
PL4-A	6.35	6.350	11	6.364	14	6.430	6.450	0
PL4-A	5.30	5.310	11	5.340	30	5.390	5.410	0
PL4-B	5.20	5.200	14	5.214	14	5.280	5.300	0
PL4-B	3.30	3.310	14	3.338	28	3.390	3.410	0
PL4-B	4.35	4.350	14	4.364	14	4.430	4.450	0
PL4-B	2.30	2.360	14	2.386	26	2.440	2.460	0
PL4-B	4.20	4.200	14	4.214	14	4.280	4.300	0
PL4-B	5.35	5.350	14	5.364	14	5.430	5.450	0
PL4-B	6.30	6.310	14	6.338	28	6.390	6.410	0
PL4-C	5.20	5.200	17	5.214	14	5.280	5.300	0
PL4-C	6.30	6.322	17	6.352	30	6.402	6.422	0
PL4-C	2.35	2.350	17	2.364	14	2.430	2.450	0
PL4-C	5.30	5.325	17	5.352	27	5.405	5.425	0
PL4-C	4.20	4.200	17	4.214	14	4.280	4.300	0
PL4-C	7.35	7.350	17	7.364	14	7.430	7.450	0
PL4-C	5.30	5.305	17	5.317	12	5.385	5.405	0

5) TEST RESULTS FOR PHASE LOSS AFTER RELAY LOCATION WHEN THE MOTOR IS RUNNING IN THE TRANSIENT MODE

The proposed scheme is tested for several cases of phase loss after the relay location, when the motor is running at the beginning, and during the transient mode. It has been found that the proposed scheme is able to detect and classify all types of these faults correctly in 1.5 cycles (30 ms) from the fault inception time. Figure 12 shows one of these cases, in which the motor is started at a time of 4.2 seconds without rotation because of the loss of phase "A" after the relay location. It is clear from this figure that the fault was detected and classified correctly (PL = 11) at a time of 4.214 seconds, and then the motor goes to a standstill. Thus, the operation time for detecting and classifying the fault is 14 ms from the fault inception time. To fully describe the performance of the proposed scheme, the fault in the simulation is quickly repaired at 4.28 sec., and then the restart button is quickly pushed at 4.3 sec. It is clear from this figure that once the restart push-button is pushed after the fault is repaired, the output of the proposed scheme returns to its normal mode and becomes zero. Table 8 gives all cases (21 cases) of this type of fault, which is known as codes PL4-A, PL4-B, and PL4-C, as previously given in Table 4.

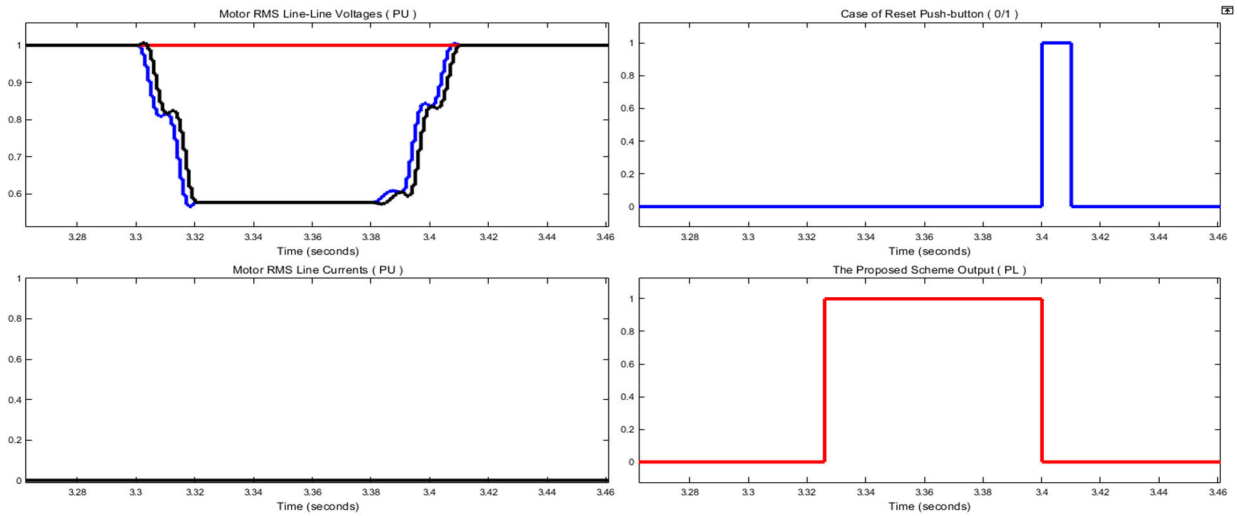

FIGURE 13. Test result of the proposed fault detector and classifier for loss of phase "A" from the power supply source at a time of 3.3 seconds when the motor is in standstill mode.

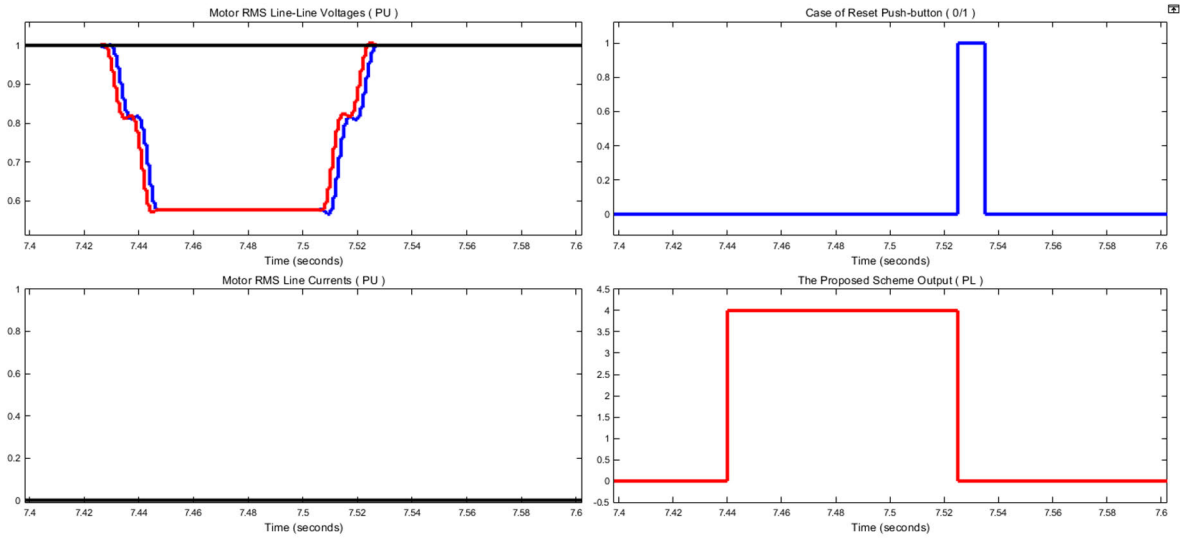

FIGURE 14. Test result of the proposed fault detector and classifier for loss of phase "B" from the power supply source at a time of 7.425 seconds when the motor is in standstill mode.

6) TEST RESULTS FOR PHASE LOSS FROM THE SOURCE WHEN MOTOR IS IN STANDSTILL MODE

The proposed scheme is tested for many cases at different times of phase loss from the source when the motor is in standstill mode. It has been found that the proposed scheme is able to detect and classify all types of these faults correctly in 1.5 cycles from the fault inception time. This type of fault is known as codes PL5-A, PL5-B, and PL5-C, as previously given in Table 4.

Figure 13 shows one of these cases, which is the loss of phase "A" of the power supply at a time of 3.3 seconds when the motor is in standstill mode. It is clear from this figure that the fault was detected and classified correctly (PL = 1) at a time of 3.326 seconds. Thus, the operation time is 26 ms from the fault inception time. To fully describe the performance of the proposed scheme, the fault in the simulation is quickly repaired at 3.38 seconds and then the restart button is quickly pushed at 3.4 seconds. It is also clear that once the restart push-button is pushed after the fault is repaired, the output of the proposed scheme returns to its normal mode and becomes zero.

Figure 14 shows another case, which is the loss of phase "B" of the power supply at a time of 7.425 seconds when the motor is in standstill mode. It is clear from this figure that the fault was detected and classified correctly (PL = 4) at a time of 7.44 sec. Thus, the operation time is 15 ms from the fault inception time. The fault in the simulation is quickly repaired at 7.505 sec., and then the restart button is quickly pushed at 7.525 sec. It is also clear that once the restart push-button is pushed after the fault is repaired, the output of

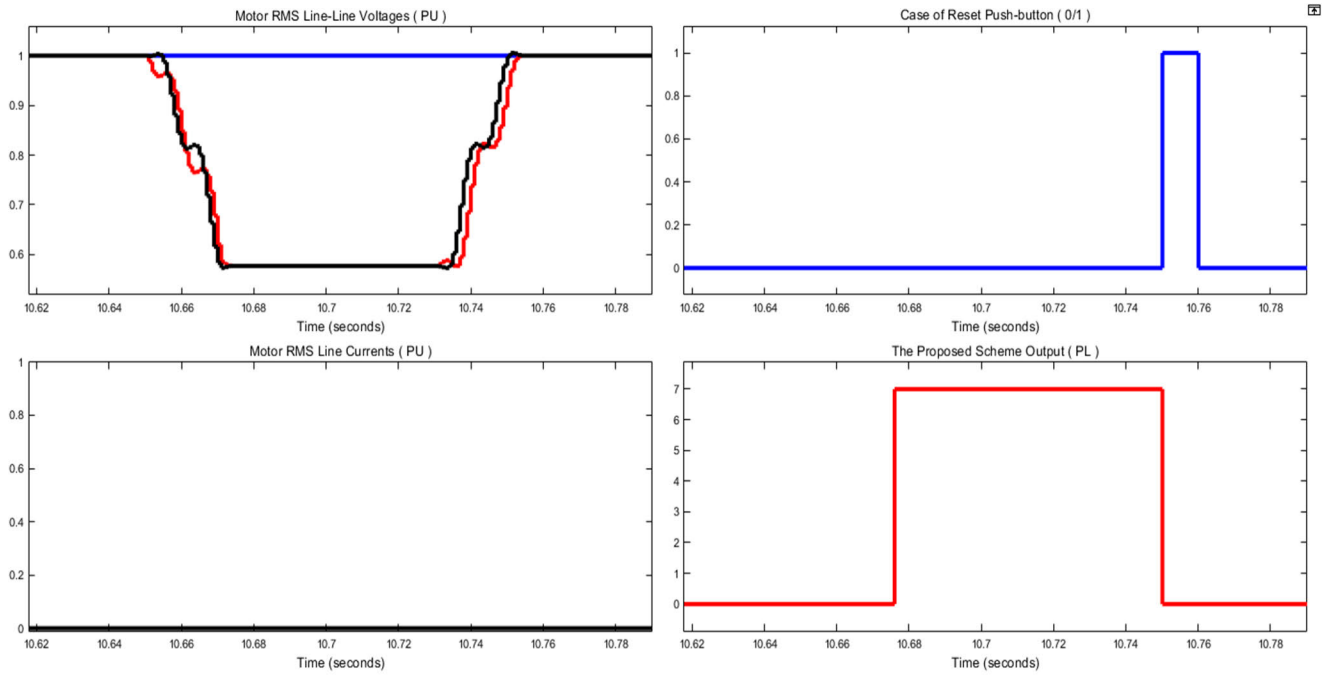

FIGURE 15. Test result of the proposed fault detector and classifier for loss of phase "C" from the power supply source at a time of 10.65 seconds when the motor is in standstill mode.

TABLE 9. Data for some different motor models present in a MATLAB Simulink environment.

Motor Parameter	Motor No.1	Motor No.2	Motor No.3	Motor No.4
Nominal power (HP)	10	50	100	150
RMS Line to Line voltage (V)	400	400	400	400
Motor Speed (RPM)	1440	1480	1484	1487
Frequency (Hz)	50	50	50	50
Pole pairs	2	2	2	2
Stator resistance Rs (Ω)	0.7384	0.08233	0.03552	0.02155
Stator inductance Ls (H)	0.003045	0.000724	0.000335	0.000226
Rotor resistance referred to stator Rr' (Ω)	0.7402	0.0503	0.02092	0.01231
Rotor inductance referred to stator Lr' (H)	0.003045	0.000724	0.000335	0.000226
Mutual inductance Lm (H)	0.1241	0.02711	0.0151	0.01038

the proposed scheme returns to its normal mode and becomes zero.

Figure 15 shows the third case, which is the loss of phase "C" of the power supply at a time of 10.65 seconds when the motor is in standstill mode. It is clear from this figure that the fault was detected and classified correctly (PL = 7) at a time of 10.676 sec. Thus, the operation time is 26 ms from the fault inception time. The fault in the simulation is quickly repaired at 10.73 sec., and then the restart button is quickly pushed at 10.75 sec. It is also clear that once the restart push-button is pushed after the fault is repaired, the output of the proposed scheme returns to its normal mode and becomes zero.

7) TEST RESULTS OF THE PHASE LOSS FAULT FOR DIFFERENT TYPES OF 3-PH INDUCTION MOTORS

One of the main advantages of the proposed scheme is that it is suitable for many motors because it is based on the per-unit values of both the RMS line-to-line voltages and the line currents of the motor. So, in this part, the presented scheme is tested under phase loss faults for some different motor models present in a MATLAB/Simulink environment. The data for these motors used in MATLAB/Simulink is given in Table 9. In the case of each motor simulation, the proposed scheme is used with different input values. The inputs of the proposed scheme used with each motor are the per-unit values of RMS line-to-line voltages and the per-unit values of RMS line currents based on the motor rating data. The test results for various cases of phase loss at full load for motors No. 1, 2, 3, and 4 are given in Tables 10, 11, 12 and 13, respectively. The proposed scheme has been tested under normal conditions, under different phase loss faults, during and after disconnecting the motor, and after pressing the restart button. The results show that the proposed scheme is able to detect and classify these faults

TABLE 10. Results of the proposed fault detector and classifier for various cases of phase loss at full load for motor No. 1 (10 HP) present in a MATLAB/Simulink environment.

Fault type code	Motor starting time (Sec.)	Fault inception time (Sec.)	Output of the proposed scheme (PL)	Fault detection time (Sec.)	Operation time (ms)	Fault repair time (Sec.)	Reset time (Sec.)	The scheme output after Reset (PL)
PL1-A	0.25	4.00	3	4.020	20	4.08	4.10	0
PL1-B	0.25	5.00	6	5.023	23	5.08	5.10	0
PL1-C	0.25	6.00	9	6.027	27	6.08	6.10	0
PL2-A	0.25	7.00	12	7.026	26	7.08	7.10	0
PL2-B	0.25	8.00	15	8.028	28	8.08	8.10	0
PL2-C	0.25	9.00	18	9.029	29	9.08	9.10	0
PL3-A	5.25	5.25	2	5.261	11	5.33	5.35	0
PL3-B	6.35	6.36	5	6.388	28	6.44	6.46	0
PL3-C	7.25	7.25	8	7.266	16	7.33	7.35	0
PL4-A	8.25	8.25	11	8.261	11	8.33	8.35	0
PL4-B	9.35	9.36	14	9.389	29	9.44	9.46	0
PL4-C	5.25	5.25	17	5.261	11	5.33	5.35	0
PL5-A	---	4.30	1	4.326	26	4.38	4.40	0
PL5-B	---	5.35	4	5.379	29	5.43	5.45	0
PL5-C	---	6.60	7	6.626	26	6.68	6.70	0

TABLE 11. Results of the proposed fault detector and classifier for various cases of phase loss at full load for motor No. 2 (50 HP) present in a MATLAB Simulink environment.

Fault type code	Motor starting time (Sec.)	Fault inception time (Sec.)	Output of proposed scheme (PL)	Fault detection time (Sec.)	Operation Time (ms)	Fault repair time (Sec.)	Reset Time (Sec.)	The scheme output after Reset (PL)
PL1-A	0.30	6.00	3	6.027	27	6.08	6.10	0
PL1-B	0.30	7.00	6	7.023	23	7.08	7.10	0
PL1-C	0.30	8.00	9	8.027	27	8.08	8.10	0
PL2-A	0.30	9.00	12	9.025	25	9.08	9.10	0
PL2-B	0.30	5.00	15	5.029	29	5.08	5.10	0
PL2-C	0.30	7.00	18	7.028	28	7.08	7.10	0
PL3-A	5.30	5.30	2	5.311	11	5.38	5.40	0
PL3-B	6.30	6.31	5	6.326	16	6.39	6.41	0
PL3-C	7.30	7.30	8	7.316	16	7.38	7.40	0
PL4-A	8.30	8.30	11	8.311	11	8.38	8.40	0
PL4-B	9.40	9.41	14	9.438	28	9.49	9.51	0
PL4-C	5.30	5.30	17	5.311	11	5.38	5.40	0
PL5-A	---	6.50	1	6.526	26	6.58	6.60	0
PL5-B	---	7.50	4	7.529	29	7.58	7.60	0
PL5-C	---	8.50	7	8.526	26	8.58	8.60	0

TABLE 12. Results of the proposed fault detector and classifier for various cases of phase loss at full load for motor No. 3 (100 HP) present in a MATLAB/Simulink environment.

Fault type code	Motor starting time (Sec.)	Fault inception time (Sec.)	Output of proposed scheme (PL)	Fault detection time (Sec.)	Operation Time (ms)	Fault repair time (Sec.)	Reset Time (Sec.)	The scheme output after Reset (PL)
PL1-A	0.30	7.00	3	7.026	26	7.08	7.10	0
PL1-B	0.30	8.00	6	8.023	23	8.08	8.10	0
PL1-C	0.30	9.00	9	9.027	27	9.08	9.10	0
PL2-A	0.30	7.00	12	7.025	25	7.08	7.10	0
PL2-B	0.30	8.00	15	8.030	30	8.08	8.10	0
PL2-C	0.30	9.00	18	9.028	28	9.08	9.10	0
PL3-A	5.40	5.40	2	5.411	11	5.48	5.50	0
PL3-B	6.40	6.41	5	6.425	15	6.49	6.51	0
PL3-C	7.40	7.40	8	7.416	16	7.48	7.50	0
PL4-A	8.40	8.40	11	8.411	11	8.48	8.50	0
PL4-B	9.40	9.41	14	9.437	27	9.49	9.51	0
PL4-C	5.40	5.40	17	5.411	11	5.48	5.50	0
PL5-A	---	3.40	1	3.426	26	3.48	3.50	0
PL5-B	---	4.50	4	4.529	29	4.58	4.60	0
PL5-C	---	5.60	7	5.626	26	5.68	5.70	0

correctly within 1.5 cycles (30 ms) from the fault's inception time.

IV. FEATURES, LIMITATION AND FUTURE WORK

In the case of designing a protection system for three-phase motors, it is necessary to consider the safety issues associated with this system by validating its performance by knowing its response speed and accuracy in detecting and classifying faults under different conditions. Therefore, many tests were conducted for the proposed scheme under normal operating conditions and various phase loss faults at different times and load conditions. The simulation results show that the

TABLE 13. Results of the proposed fault detector and classifier for various cases of phase loss at full load for motor No. 4 (150 HP) present in a MATLAB/Simulink environment.

Fault type code	Motor starting time (Sec.)	Fault inception time (Sec.)	Output of proposed scheme (PL)	Fault detection time (Sec.)	Operation Time (ms)	Fault repair time (Sec.)	Reset Time (Sec.)	The scheme output after Reset (PL)
PL1-A	0.20	7.00	3	7.027	27	7.08	7.10	0
PL1-B	0.20	8.00	6	8.023	23	8.08	8.10	0
PL1-C	0.20	9.00	9	9.027	27	9.08	9.10	0
PL2-A	0.20	7.00	12	7.025	25	7.08	7.10	0
PL2-B	0.20	8.00	15	8.030	30	8.08	8.10	0
PL2-C	0.20	9.00	18	9.028	28	9.08	9.10	0
PL3-A	5.28	5.28	2	5.291	11	5.36	5.38	0
PL3-B	6.28	6.30	5	6.321	21	6.38	6.40	0
PL3-C	7.28	7.28	8	7.296	16	7.36	7.38	0
PL4-A	7.28	7.28	11	7.291	11	7.36	7.38	0
PL4-B	6.28	6.30	14	6.327	27	6.38	6.40	0
PL4-C	5.28	5.28	17	5.291	11	5.36	5.38	0
PL5-A	---	3.30	1	3.326	26	3.38	3.40	0
PL5-B	---	4.40	4	4.429	29	4.48	4.50	0
PL5-C	---	5.50	7	5.526	26	5.58	5.60	0

proposed scheme can correctly detect and classify phase loss faults within 30 ms of the fault inception time. As a result, the proposed scheme detects these faults within a short time of their occurrence. Thus, the motor is quickly disconnected when this fault occurs, which ensures the safety of the motor from burning its coils, the nearby people and other equipment associated with this system.

It is worth noting that the long-term reliability of any protection system depends on several factors, such as the overall system design, component quality, installation quality, maintenance, and operational practices. Regarding the design, the proposed system was designed to detect and classify 15 types of faults that can occur due to the phase loss of a three-phase induction motor. Then it tested for more than 87 cases under normal conditions and phase loss faults at different conditions. Also, it tested for other cases (60 different cases) of phase loss faults for four different motor models. All test results showed that the proposed scheme is reliable and works highly efficiently in detecting and classifying phase loss faults for a three-phase induction motor when the motor runs in the steady and transient modes and when it is in the standing mode.

From an economic standpoint, the proposed scheme is considered more effective and acceptable compared to traditional protection systems in detecting and diagnosing this fault. It can be applied to most motors, regardless of their size. However, the economic return on reducing downtime, predicting motor failures, and reducing maintenance costs will be more beneficial for larger motors.

Most of the phase loss faults of a three-phase induction motor are in only one phase, so the proposed scheme is designed to detect this fault and thus disconnect the motor. Multi-phase loss faults are rare, and if this happens in two phases simultaneously, this does not represent a danger to the motor because it will disconnect as soon as two phases are lost from its source. Unlike single-phase faults, they cause an increase in currents in the two correct phases, which increases the motor's temperature and can lead to the burning of the motor windings. In future work, it is possible to consider improving the protection system by designing an effective protection system to detect and classify most faults of 3-phase induction motor in addition to multi-phase faults. Thus, the proposed scheme can be integrated into the overall protection system for 3-phase induction motor.

V. CONCLUSION

This paper proposes an efficient protection scheme to detect and classify 15 types of phase loss faults for a three-phase IM. These faults are classified according to the unhealthy phase, fault location either from the power source or beyond the relay point, and motor action modes (standstill mode, transient mode, and steady state mode). Several tests have been performed to evaluate the proposed scheme's performance. With the help of Simulink in Matlab software, the proposed method with a motor model of 20 hp has been simulated and tested for more than 87 different cases under normal conditions and phase loss faults at different conditions. One of the advantages of the presented method is its suitability for many motors because the inputs to the proposed scheme are the per-unit values of both RMS line-line voltages and line currents. So, the presented scheme is tested for many other cases (60 different cases) of phase loss faults for 4 different motor models present in a MATLAB/Simulink environment. To fully illustrate the performance of the proposed scheme, it has been tested under normal conditions and under different faults for phase loss, during and after disconnecting the motor, and after pushing the restart button. All simulation results show that the proposed scheme works with high efficiency and is able to detect and correctly classify phase loss faults for 3-phase IM within 1.5 cycles (30 ms) of the fault inception. Thus, the proposed scheme can be used as a simple and reliable scheme in the protection system of a 3-phase IM to detect and classify the types of phase loss faults.

DATA AVAILABILITY

The data used to support the findings of this study are available from the corresponding author upon request.

DECLARATION OF COMPETING INTEREST

The authors declare that they have no known competing financial interests or personal relationships that could have appeared to influence the work reported in this paper.

REFERENCES

[1] N. A. Mohar, E. C. Mid, S. M. Suboh, N. H. Baharudin, N. B. Ahamad, N. A. Rahman, E. Ruslan, and D. A. Hadi, "Fault detection analysis for three phase induction motor drive system using neural network," *J. Phys., Conf. Ser.*, vol. 1878, no. 1, May 2021, Art. no. 012039.

[2] R. S. Kumar, B. R. Kumar, and M. L. Luciana, "Fault detection for three-phase induction motor drives using fuzzy logic," *Int. J. Appl. Math.*, vol. 118, no. 20, pp. 2071–2079, 2018.

[3] U. Sengamalai, G. Anbazhagan, T. M. T. Thentral, P. Vishnuram, T. Khurshaid, and S. Kamel, "Three phase induction motor drive: A systematic review on dynamic modeling, parameter estimation, and control schemes," *Energies*, vol. 15, no. 21, p. 8260, Nov. 2022.

[4] A. Dianov and A. Anuchin, "Phase loss detection using current signals: A review," *IEEE Access*, vol. 9, pp. 114727–114740, 2021.

[5] A. Sinha and S. Grover, "Modified circuit design of VFD for critical loads under single phasing condition," *Int. J. Eng. Trends Technol.*, vol. 69, no. 6, pp. 233–238, Jun. 2021.

[6] B. Alsayid, "Experimental investigation and analysis of induction motors operation under single-phasing condition," *Palestine Tech. Univ. Res. J.*, vol. 8, no. 2, pp. 90–99, Sep. 2020.

[7] C. Bussmann, "Motor protection voltage unbalance and single-phasing," *Duke Energy Prog.*, Nov. 2014. [Online]. Available: https://tinyurl.com/23k79t8y

[8] K. Vishnu and Y. Alekhya, "Single phasing preventer for the protection of three phase faults," *J. Emerg. Technol. Innov. Res.*, vol. 9, no. 2, pp. 236–239, 2022.

[9] D. S. Batorowicz, J. Hanson, O. Goieva, W. Schoenberger, and A. Shustov, "Impact of open phase fault conditions on electrical protection and motor behaviour," in *Proc. 13th Int. Conf. Develop. Power Syst. Protection (DPSP)*, Edinburgh, U.K., Mar. 2016.

[10] P. Aree, "Effects of neutral conductor on induction motor steady-state performance under loss of one phase of supply voltages," in *Proc. 2nd IEEE Int. Conf. Power Electron., Intell. Control Energy Syst. (ICPEICES)*, Oct. 2018, pp. 837–840.

[11] F. J. T. E. Ferreira, A. M. Silva, and A. T. de Almeida, "Single-phasing protection of line-operated motors of different efficiency classes," *IEEE Trans. Ind. Appl.*, vol. 54, no. 3, pp. 2071–2084, May 2018.

[12] *Excessive Heat in Electric Motors*, Megger Company, Dover, U.K., 2022. [Online]. Available: https://n9.cl/0nhyj

[13] Y. Mollet, M. Pergolesi, M. Sarrazin, K. Janssens, H. Van der Auweraer, P. Chiariotti, P. Castellini, and J. Gyselinck, "Multi-physical signature analysis of induction machines under unbalanced supply voltage," in *Proc. 8th Int. Conf. Electr. Mach. (ICEM)*, Sep. 2018, pp. 2378–2384.

[14] A. H. Jassim, A. A. Hussein, and L. F. Abbas, "The performance of a three-phase induction motor under and over unbalance voltage," *Tikrit J. Eng. Sci.*, vol. 28, no. 2, pp. 15–32, Jul. 2022.

[15] J. Hang, X. Ren, C. Tang, M. Tong, and S. Ding, "Fault-tolerant control strategy for five-phase PMSM drive system with high-resistance connection," *IEEE Trans. Transport. Electrific.*, vol. 7, no. 3, pp. 1390–1400, Sep. 2021.

[16] A. Dianov, "A novel phase loss detection method for low-cost motor drives," *IEEE Trans. Power Electron.*, vol. 37, no. 6, pp. 6660–6668, Jun. 2022.

[17] A. Dianov and A. Anuchin, "Phase loss detection using voltage signals and motor models: A review," *IEEE Sensors J.*, vol. 21, no. 23, pp. 26488–26502, Dec. 2021.

[18] I. Z. Giceva, V. J. Sarac, S. A. Gelev, and V. T. Cingoski, "Single phasing of three phase induction motors under various load conditions," in *Proc. 23rd Int. Sci.-Prof. Conf. Inf. Technol. (IT)*, Feb. 2018, pp. 1–4.

[19] R. Mulindwa, *Protecting 3 Phase Motors From Single Phasing*. Kampala, Uganda: Makerere Universty, 2019.

[20] P. Singh, R. N. Dash, and C. K. Panigrahi, "Open phase fault analysis of a three-phase induction motor," in *Proc. Int. Conf. Emerg. Trends Adv. Elect. Eng. Renew. Energy*. Cham, Switzerland: Springer, 2021, pp. 81–89.

[21] A. Boum, N. J. Maurice, L. N. Nneme, and L. M. Mbumda, "Fault diagnosis of an induction motor based on fuzzy logic, artificial neural network, and hybrid system," *Int. J. Control*, vol. 8, no. 2, pp. 42–51, 2018.

[22] C. Boopathi, S. Chowdhary, and S. Karn, "Three phase induction motor protection using embedded technology," *Int. J. Electr. Eng. Technol.*, vol. 11, no. 3, pp. 1–8, 2020.

[23] A. A. Obed, "Detection, protection from, classification, and monitoring of electrical faults in 3-phase induction motors based on discrete S-transform," *Int. J. Appl. Eng. Res.*, vol. 13, no. 9, 2018, pp. 6690–6699.

[24] S. Prabakaran and S. Venkatesan, "Analysis of 3 phase induction motor protection using numerical relay," *Int. J. Eng. Tech.*, vol. 4, pp. 513–519, Mar. 2018.

[25] S. A. Saleh, J. Meng, E. Ozkop, M. E. Valdes, T. Hill, and A. Al-Durra, "Impacts of the sampling rate on responses of digital protective relays," in *Proc. IEEE/IAS 59th Ind. Commercial Power Syst. Tech. Conf. (I&CPS)*, Las Vegas, NV, USA, May 2023, pp. 1–9.

[26] X. Zhang, Y. Hu, J. Deng, H. Xu, and H. Wen, "Feature engineering and artificial intelligence-supported approaches used for electric powertrain fault diagnosis: A review," *IEEE Access*, vol. 10, pp. 29069–29088, 2022.

[27] Z. Liu, A. Houari, M. Machmoum, M. F. Benkhoris, and T. Tang, "A second order filter-based fault detection method for five-phase permanent magnet synchronous generators," in *Proc. IECON 46th Annu. Conf. IEEE Ind. Electron. Soc.*, Oct. 2020, pp. 4827–4832.

[28] S.-C. Yang, Y.-L. Hsu, P.-H. Chou, D.-R. Jian, and G.-R. Chen, "Comparison of open-phase fault detection for permanent magnet machine drives using different fault signals," in *Proc. IEEE Energy Convers. Congr. Exposit. (ECCE)*, Oct. 2017, pp. 385–390.

[29] A. Dianov and A. Anuchin, "Fast square root calculation for control systems of power electronics," in *Proc. 23rd Int. Conf. Electr. Mach. Syst. (ICEMS)*, Nov. 2020, pp. 438–443.

[30] M. J. Duran, I. Gonzalez-Prieto, N. Rios-Garcia, and F. Barrero, "A simple, fast, and robust open-phase fault detection technique for six-phase induction motor drives," *IEEE Trans. Power Electron.*, vol. 33, no. 1, pp. 547–557, Jan. 2018.

[31] M. A. Zdiri, B. Bouzidi, and H. H. Abdallah, "Improved diagnosis method for VSI fed IM drives under open IGBT faults," in *Proc. 15th Int. Multi-Conf. Syst., Signals Devices (SSD)*, Mar. 2018, pp. 905–910.

[32] H. Yan, Y. Xu, F. Cai, H. Zhang, W. Zhao, and C. Gerada, "PWM-VSI fault diagnosis for a PMSM drive based on the fuzzy logic approach," *IEEE Trans. Power Electron.*, vol. 34, no. 1, pp. 759–768, Jan. 2019.

[33] R. Maamouri, M. Trabelsi, M. Boussak, and F. M'Sahli, "Mixed model-based and signal-based approach for open-switches fault diagnostic in sensorless speed vector controlled induction motor drive using sliding mode observer," *IET Power Electron.*, vol. 12, no. 5, pp. 1149–1159, May 2019.

[34] V. F. Pires, T. G. Amaral, A. Cordeiro, D. Foito, A. J. Pires, and J. F. Martins, "Fault-tolerant SRM drive with a diagnosis method based on the entropy feature approach," *Appl. Sci.*, vol. 10, no. 10, p. 3516, May 2020.

[35] S. Xu, J. Wang, and M. Ma, "Open-circuit fault diagnosis method for three-level neutral point clamped inverter based on instantaneous frequency of phase current," *Energy Convers. Econ.*, vol. 1, no. 3, pp. 264–271, Dec. 2020.

[36] M. Yakovenko, A. Anuchin, V. Ostrirov, and K. Milskiy, "Implementation of a protected low-cost voltage-source inverter," in *Proc. 10th Int. Conf. Electr. Power Drive Syst. (ICEPDS)*, Oct. 2018, pp. 1–4.

[37] M. Rahnama, A. Vahedi, A. Mohammad-Alikhani, and N. Takorabet, "Terminal voltage harmonic analysis of brushless synchronous generator for fault detection," in *Proc. Int. Conf. Electr. Mach. (ICEM)*, vol. 1, Aug. 2020, pp. 1445–1451.

[38] J. Hang, S. Ding, J. Zhang, M. Cheng, and Q. Wang, "Open-phase fault detection in delta-connected PMSM drive systems," *IEEE Trans. Power Electron.*, vol. 33, no. 8, pp. 6456–6460, Aug. 2018.

AHMED DAWOOD received the M.Sc. degree in electrical engineering from the Faculty of Engineering in Cairo, Al Azhar University, Egypt, in 2017, where he is currently pursuing the Ph.D. degree with the Department of Electrical Power and Machines. He is an Assistant Lecturer with the Department of Electrical Engineering, Faculty of Engineering in Qena, Al Azhar University. His research interests include power system protection, electrical energy economics, AI techniques, PLCs, and SCADA systems.

MOHAMED A. ISMEIL (Member, IEEE) was born in Qena, Egypt, in October 1977. He received the B.Sc. and M.Sc. degrees in electrical engineering from South Valley University, in 2002 and 2008, respectively, and the Ph.D. degree from the Channel System Program, Aswan University, in April 2014. From October 2010 to January 2013, he was a Ph.D. Student with the Department of Electrical Drive Systems and Power Electronics, Technical University of Munich, Germany. From April 2014 to September 2018, he was an Assistant Professor with the Aswan Faculty of Engineering, Aswan University. Since October 2018, he has been an Associate Professor with the Faculty of Engineering, South Valley University. From March 2020 to November 2022, he was the Head of the Electrical Department, Faculty of Engineering at Qena. Since November 2022, he has been an Associate Professor with the College of Engineering, King Khalid University, Saudi Arabia. He has published more than 45 papers in international conferences and journals. His current research interests include power electronics applications in wind energy conversion systems, PV interface with the utility, smart grid technologies, digital control applications (PIC, FPGA, and DSP), and protection. His main interest is power inverter design for renewable applications.

HANY S. HUSSEIN (Senior Member, IEEE) received the B.Sc. degree in electrical engineering and the M.Sc. degree in communication and electronics from South Valley University, Egypt, in 2004 and 2009, respectively, and the Ph.D. degree in communication and electronics engineering from the Egypt–Japan University of Science and Technology (E-JUST), in 2013. In 2012, he was a special Researcher Student with Kyushu University, Japan. He has been an Associate Professor with the Faculty of Engineering, Aswan University, since 2019. He is currently an Assistant Professor with the College of Engineering, King Khalid University, Saudi Arabia. His research interests include digital signal processing for communications, multimedia, image, video coding, and low-power wireless communications. He is a technical committee member of many international conferences and a reviewer of many international conferences, journals, and transactions. He was the General Co-Chair of the IEEE ITCE, in 2018.

B. M. HASANEEN received the B.Sc., M.Sc., and Ph.D. degrees in electrical engineering from the Faculty of Engineering in Cairo, Al Azhar University, Egypt. He was the Dean of the Faculty of Engineering in Qena for more than 12 years. He has been a Professor with the Department of Electrical Power and Machine Engineering, Faculty of Engineering in Qena, Al-Azhar University. His current research interests include electrical machines, control, and solar energy.

A. M. ABDEL-AZIZ was born in Alexandria, Egypt, in 1940. He received the B.Sc. degree in electrical power engineering from Alexandria University, in 1963, and the Dipl.-Ing. and Dr.-Ing. degrees in electrical engineering from the Technical University of Braunschweig, Germany, in 1968 and 1972, respectively. He is currently a Professor of power systems with the Department of Electrical Power and Machines, Faculty of Engineering, Al-Azhar University, Cairo, Egypt. His current research interests include protection, HV, and solar energy. He is a member of the Egyptian Committee for the Code of Electrical Installations in Buildings, Housing, and Building National Research Centre (HBRC), Ministry of Housing.